Babeș-Bolyai University, Cluj-Napoca

Faculty of Geography

Doctoral School of Geography

DOCTORAL THESIS

SPATIAL ANALYSIS MODELS FOR DIGITAL MAPPING OF AREAS VULNERABLE TO FLASH FLOODS WITHIN TORRENTIAL BASINS. CASE STUDIES IN THE OAȘ-GUTÂI-ȚIBLEȘ MOUNTAIN GROUP

- summary -

Scientific supervisor:

Prof. univ. dr. Ioan-Aurel IRIMUȘ

PhD candidate:

István KOCSIS

CLUJ-NAPOCA

2023

CONTENT

KEYWORDS: flash flood; torrential watershed; vulnerability; GIS model; spatial interpolation; meteorological radar; rain gauge, hydrological station; spatial analysis; bivariate statistical analysis; FFPI; hydrological modelling; frequency analysis.

1. INTRODUCTION

The risk associated with extreme hydrological processes (flash floods, floods) is more present than ever, taking into account the global climatic changes, the expansion of inhabited areas, and the changes emerging as a result of inadequate land management. Of all the hydrological risks, slope flash floods represent the processes with the highest impact because of the high speed of their development and their place of origin, making them difficult to predict. Due to the ever-increasing intensity and frequency of slope floods, makes the need to prepare hazard and vulnerability studies related to them increasingly important.

Floods in general represent a natural hazard that causes significant damage, the effects of which can be mitigated through integrated flood risk management. Reducing the effects of these disasters involves the interdisciplinary study of hazards, vulnerability, and risk, respectively information and awareness of the population (Dimitrie Cantemir University, 2013).

Spatial analysis and digital mapping of hydro-meteorological phenomena cannot be achieved without modern means such as specialized applications, web resources, field measurement tools, and remote sensing for land surface investigation. The development of geographic sciences is based on the arsenal of methods and tools offered by GIS technologies (Irimuş et al., 2005), thus acquiring a complex and indispensable role in the presentation and description of hydrological processes, such as slope floods.

Through this paper, we propose the development and presentation of spatial analysis models based on statistical and empirical analysis, in order to identify areas susceptible to flash floods, by presenting the territorial vulnerability, classified into five classes, from very low to very high vulnerability; respectively highlighting the effects that the intensification of land use has on the surface runoff in the studied hydrographic basins (h.b.).

1.1. MOTIVATION FOR THE SELECTION OF THE RESEARCH TOPIC

Throughout my profession as a hydrologist in the field of water management within the Someș-Tisa Water Brach, I had the opportunity to meet and face the dangerous meteorological phenomena that lead to the occurrence and development of hydrological events with the risk of flooding, respectively of flash floods. Experiencing these events and knowing the existing deficiencies in flood prevention and protection measures, I identified the necessity to develop effective studies to support the identification of areas vulnerable to flash floods and implicitly in the management of emergency situations.

1.2. RESEARCH OBJECTIVES

As it appears from the title, the main objective of the research theme is the digital mapping of areas vulnerable to flash floods, within the torrential hydrographic basins of the Oaș-Gutâi-Țibleș Mountain group.

In the process of achieving the proposed object, a series of complementary objectives were fulfilled by implementing several spatial analysis methodologies, statistical analysis methods, respectively hydrological modeling, with the aim to highlight the role and importance of the degree of accuracy of the databases used, both numerical and spatial ones, concretized and validated by developing case studies:

- carrying out a comparative analysis on the amounts of precipitation recorded at meteorological stations in the area of the Someș-Tisa hydrographic basin, with those observed by meteorological radars;
- the presentation of the GIS methodology for correcting the amounts of rainfall estimated by radar, based on in situ measurements, in order to spatialize the rainfall in the area of the Țibleș and Rodnei Mountains;
- performing statistical analysis in order to determine the frequency and intensity of flash floods in the Valea Rea River basin;
- carrying out a study with the aim to analyze the influence of changes in vegetation cover over time, on surface runoff;
- the achievement of a GIS methodology based on the WofE bivariate statistical analysis model, in order to create the flood susceptibility map, in the Valea Rea River basin;
- physical validation of the results obtained with the GIS model, based on the hydrological modeling of a flash flood produced inside the upper hydrographic basin of the Valea Rea River.

2. ELEMENTS OF GEOGRAPHICAL LOCATION OF THE STUDY AREA

The study area of the doctoral thesis is located in the Maramureș Carpathians, part of the Northern Group of the Eastern Carpathians, being delimited by the Oaș-Gutâi-Țibleș group of volcanic mountains, developed during the Neogene volcanic manifestations, respectively by the Rodnei Mountains. In order to study the slope floods, two distinct hydrographic basins were selected, developed on the southern slope of the mentioned mountains, these being: the Valea Rea hydrographic basin and the Țibleș-Runc-Sălăuța hydrographic basin *(Figure 1)*.

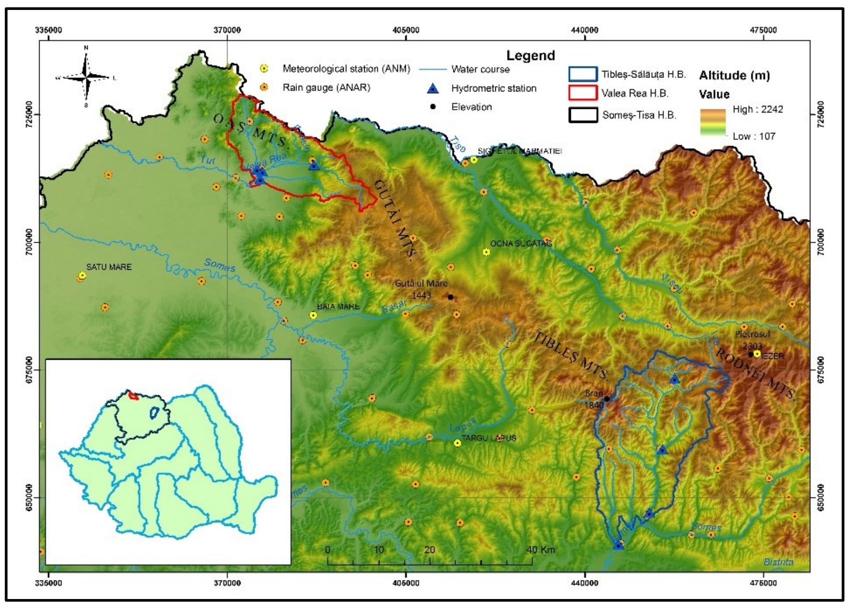

Figure 1. Geographical location of the study area

When selecting these hydrographic basins, the following criteria were taken into consideration: the surface of the hydrographic sub-basins should not be greater than 100 km^2; the frequency of flash floods in the last decade; the existence of the monitoring network, of an automatic hydrometric station for recording level increases; availability of hydro-meteorological data and their accuracy; the existence of human settlements; the complexity of the physical-geographical factors, the observation of several relief steps.

3. THE STATE OF KNOWLEDGE OF THE RESEARCH TOPIC AT THE NATIONAL AND INTERNATIONAL LEVEL. CURRENT INVESTIGATION METHODS AND TECHNIQUES

In this chapter are presented GIS methods and techniques used both nationally and internationally to calculate and improve parameters representing the input data in hydrological models for simulating flash floods, the spatial analysis methods for identifying territorial vulnerability classes, respectively stochastics models specific to the representation of the hydrological series, in order to determine the probability of occurrence of the maximum discharge generating floods, respectively to determine their frequency and intensity.

Therefore, all the general aspects related to the work methods and methodologies used in the acquisition, processing, and analysis of cartographic, numerical, and geospatial data were presented, respectively in order to interpret the results obtained in different stages of work, through direct application to case studies, methods and methodologies such as:

- spatial estimation of precipitation:
  - precipitation estimation with meteorological radars
  - types of synoptic situations generating instability
  - spatial interpolation methods
  - techniques for combining different sources of precipitation
- digital mapping of areas vulnerable to flash floods
  - assessment and mapping of vulnerability to flash floods based on the FFPI index
  - analysis of the effects of land use change on surface runoff using the SCS-CN method
- modeling of flash floods and analysis of their frequency of occurrence
  - the classic methodology for calculating the maximum runoff
  - types of hydrological models

The optimal methods chosen in order to run the case studies were those that confirmed and offered the best results in the numerous works studied and developed both at the national and international levels.

4. SPATIAL ANALYSIS MODELS IMPLEMENTED FOR THE IDENTIFICATION OF PRECIPITATION GENERATING MAXIMUM DISCHARGE

The rainfall forecast is one of the most difficult, but also the most important activity for meteorology and hydrology. Although classical rain gauges provide accurate rainfall amount data the interpolation of them is difficult, especially because of the high spatial and temporal variability. On the other hand, a high-resolution type of information is highly required in hydrological modeling for discharge calculations in small catchments. This problem is partially solved by meteorological radars, which provide precipitation data with high spatial and temporal distributions.

The territory of Romania is currently monitored by seven Doppler meteorological radars, administrated by the National Meteorological Administration (ANM): five S-band WSR-98D units, two C-band EEC-2500C, and one Gematronik METEOR 500C.

The Igniș METEOR 500C hydrometeorological radar, located north of Baia Mare, is integrated with the 7 operational weather radars *(Figure 2)*.

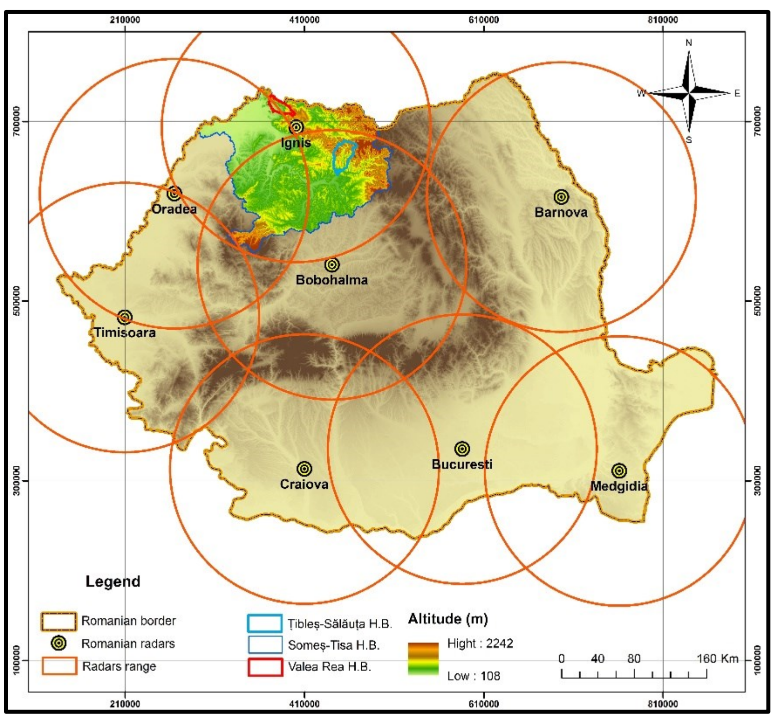

Figure 2. The National Radar Network, with a range set at 150 km

4.1. DETERMINATION OF THE PRECIPITATION POTENTIAL OF CLOUD FORMS BASED ON RADAR IMAGES

The success in choosing the optimal methods of interpolation, respectively of combining precipitation sources regarding their spatial distribution, consists in identifying and analyzing the development of synoptic situations. The present study considers the comparative analysis of the amounts of precipitation estimated by the meteorological radars WSR-98D Oradea and WSR-98D Bobohalma and those recorded at the meteorological stations/rain gauges in August 2020, with the aim of identifying the factors that lead to the presence of major differences in the precipitation field. The study area includes North-West Romania, implicitly the entire Someș-Tisa hydrographic basin.

4.1.1. Methodology and databases

For the development of the study, data on the amount of rainfall in 24 hours were used. The meteorological stations taken into analysis, in number of 15, are located in different relief conditions. Radar data were collected from the WSR (Doppler Weather Radar S-band) database, from the Oradea (RDOD) radar, located in Bihor County, and Bobohalma (RDBB) radar, located in Mureș County.

In order to carry out the case studies, we proceeded to identify the days with precipitation for 24 hours in August 2020. Out of the 31 days of August, 14 cases with precipitation were highlighted, these days being the following: 4-5, 7-8, 9-11, 15-16, 17-19, and 23-25.

For the analysis of synoptic conditions generating instability, a statistical calculation was carried out regarding the types of synoptic situations generating instability. This classification was made by consulting the *http://www.wetter3.de/Archiv/,* and *http://www.esrl.noaa.gov* archives, being consulted the synoptic maps regarding the distribution field of the geopotential height at 500 hPa level (goddam) and the distribution of the surface pressure level and associated frontal systems.

4.1.2. Results

The convective and pre-frontal synoptic conditions highlighted that both WSR-98D Oradea and Bobohalma are in correlation with the registered water amounts but with abnormalities between different areas.

Both the WSR-98D and RDBB radars provide good estimates of precipitation in the Apuseni Mountains region, for the western part of Cluj and Sălaj Counties, areas located approximately at equal distance from the two radars, between 50-150 km. On the other hand, for the eastern, more remote part of the studied area (eastern Maramureș County and northeastern Bistrița-Năsăud County), located at distances of 150-200 km, RDOD underestimates rainfall amounts, moreover omits their observation. On the contrary, RDBB has a more precise approximation for the entire study area, including for more remote areas, located at distances between 150-200 km, such as eastern Satu Mare County and Maramureș County.

4.2. CORRECTION OF RADAR-ESTIMATED PRECIPITATION AMOUNTS BASED ON IN SITU MEASUREMENTS FOR PRECIPITATION SPATIALISATION

The purpose of this study was to validate a conditional merging technique of two different sets of precipitation, applied to 15 rainfall events that occurred on the southern slope of the Țibleș and Rodnei Mountains, in Țibleș-Runc-Sălăuța h.b. A GIS methodology, based on geostatistical and spatial analysis tools was used to extract the optimal information content from the observed radar and to analyze and process them (Kocsis et al., 2022).

4.2.1. Methodology and databases

In order to combine radar and rain gauge rainfall data using the conditional merging technique (CMT) in our study area the collected data were processed through many methodological steps (*Figure 3)*.

From a methodological point of view, the research approach is based on two main stages that define a model for the integrated analysis of singular components in order to obtain the results materialized in databases useful in the flash flood modeling process. The proposed methodology involves the acquisition of databases that substantiate the model of spatial analysis through two distinct and different techniques: direct acquisition (24 h precipitation measured at rain gauges) and indirect acquisition based on spatial analysis supported by the integration of remote sensing images (24 h radar rainfall intensity).

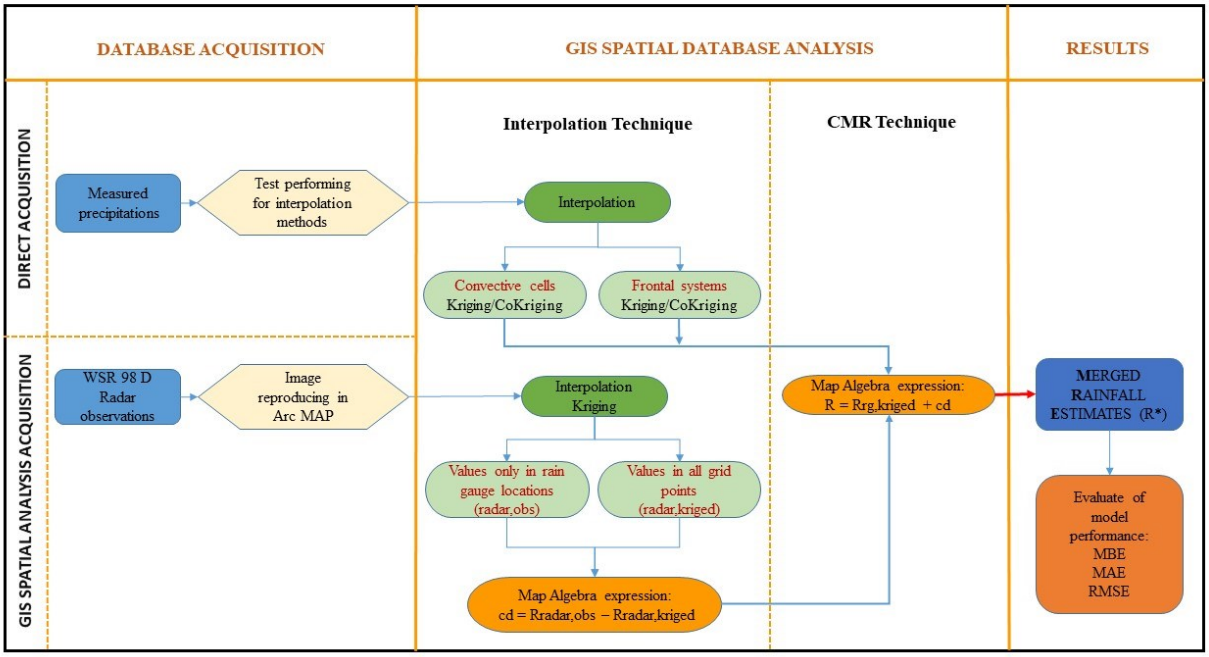

Figure 2. The scheme of the methodological workflow

The indirect acquisition of the databases within the proposed model is materialized in a submodel of spatial analysis that is validated through the databases acquired directly.

To confirm and validate the CMT of precipitation data, 15 rainfall events were selected and analyzed. The event occurred in the period of 2015-2018, from the second half of May until mid-September, in the middle sector of the Someșul Mare river basin.

Two main datasets were used in this study: 24 h precipitation measurements from 8 rain gauges from the „Romanian Waters" National Administration, Someș-Tisa Water Branch network, and 24 h rainfall intensity observations from WSR98-RDBB Bobohalma radar.

The spatial analysis stage focuses on the interpolation technique as the main method of spatializing the information provided by the input databases, which refer to the pointwise precipitation acquired, and those acquired by analyzing radar images. The interpolation of discrete precipitation values was performed using two statistical methods based on *Kriging* and *Cokriging* because, in the process of spatial analysis, the altitudes were used as a basis for precipitation variation (Kocsis et al., 2022).

The kriging family includes several interpolation methods, of which three were used in our study: *simple, ordinary kriging, and cokriging.*

Accordingly, radar information can be used to correct the interpolation of the rain gauges. The result is an estimated merged rainfall field, which preserves the radar spatial structure being conditioned at the same time using rain gauge data (Sinclair and Pegram, 2005).

The validation step was performed based on statistical analysis using three validation metrics: mean bias error (MBE), mean absolute error (MAE), and root mean square error (RMSE).

4.2.2. Results

The main database that substantiated the proposed GIS spatial analysis models is represented by radar images obtained in analog format, images that required detailed processing of the information presented, in order to obtain a database structure with high accuracy for inclusion within the proposed research methodology *(Figura 4).*

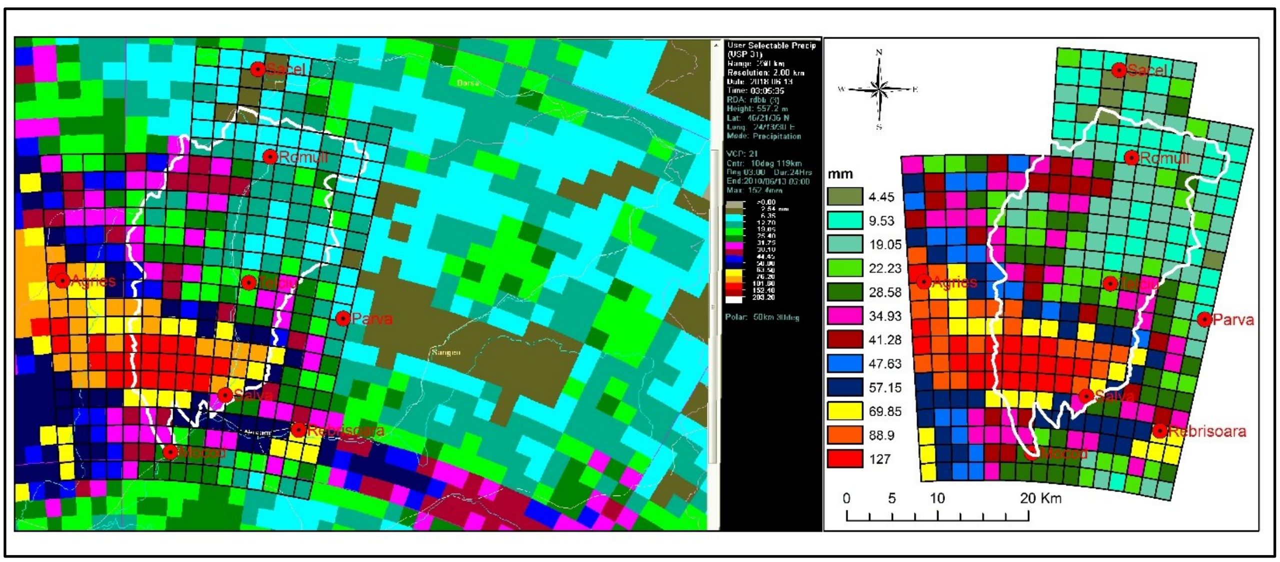

Figure 4. 24 h rain intensity radar image (left), and radar image reproduced in ArcMap (right), an event from 13 June 2018

Obtaining databases in raster format representing the averages of the observed precipitation is outlined in the initial results with a major impact within the proposed models, results obtained based on the spatial analysis of the vector structures, and the raster–vector overlay. For the spatialization of daily precipitation over 24 hours, both measured and observed by radar, we used Kriging methods, therefore simple kriging, ordinary kriging, and cokriging techniques.

The event that occurred on 13 June 2018, was selected to detail the merging process. The 24 hours accumulated rainfall estimated by the radar and interpolated from the rain gauge observations are shown in *Figures 5.a. and 5.b.* Comparing the two images, the higher spatial resolution of the radar-derived data is obvious, the precipitation distribution being much more representative of the studied event. We noticed that the area with higher rainfall values partially covered the rain gauge locations on the western extremity of the area. The radar field showed a more reliable rain distribution. In this case, the rain estimated by the radar was higher than that observed by the rain gauges.

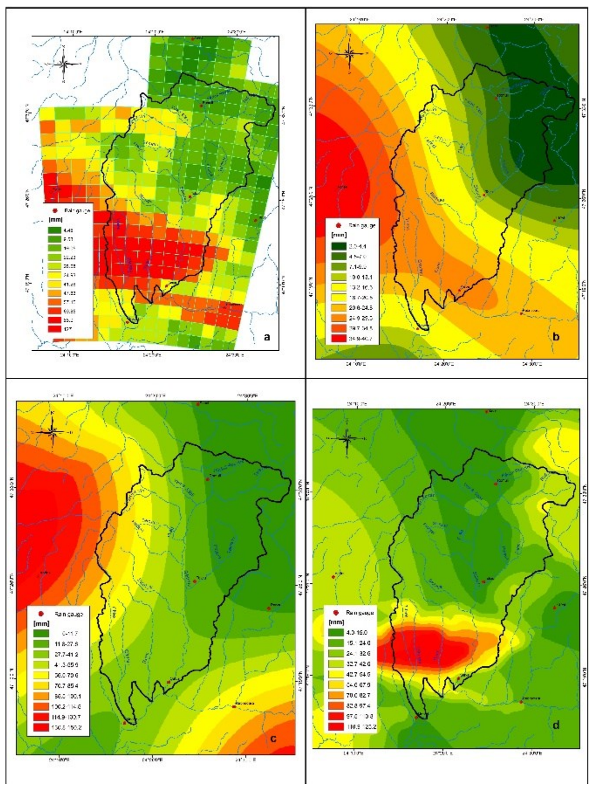

Figure 5. Conditional merging process: (a) Rainfall estimated by radar; (b) Rainfall measured by rain gauges and kriged at the resolution of the radar pixel; (c) Rainfall estimated by the radar at the rain gauge locations and kriged; (d) Final rainfall field estimated by the conditional merging technique.

Figure 5.c. shows the interpolated rain field estimated by the radar at the rain gauge locations. Upon comparing this picture with *Figure 5.b.,* the same structure may be observed, but with higher values. The final product obtained by the conditional merging technique is presented in *Figure 5.d.*

The MBE was negative in all cases, indicating that the rainfall model tended to overestimate precipitation at rain gauge locations. The lowest bias error (-2.225 mm) was associated with the rainfall event from June 16, 2016, indicating that the precipitation of this event was the most overestimated by the model among the other analyzed rainfall events. In agreement with the MBE value, the MAE (2.225 mm) and RMSE (4.188 mm) also indicated that the model is less accurate for the rainfall event on June 16, 2016. Based on the low MAE and RMSE, the model performs best in the case of rainfall events on June 3, 2018, and May 26, 2017 (both have frontal system origins).

The final high-resolution merged rainfall estimate map obtained for the 15 studied rainfall events offers a real spatial distribution of precipitation over an analyzed catchment *(Figure 6)*. It can be observed that the highest amounts of precipitation in the case of some events are discharged in the same location, or close to the rain gauges.

In the case of frontal systems rainfall events, the weather radar represents difficulties in terms of correctly estimating the precipitation values at the rain gauge points location. Although the radar detects areas with a significant load of precipitation, it tends to slightly overestimate the values compared to the measured quantities. On the other hand, in the case of convective cells rainfall events, the weather radar tends to slightly underestimate the values compared to the measured precipitation at the rain gauge points location.

Overall, we notice that the model performed very well in 11 out of 15 rainfall events (approximately 78%), with MAE under 0.4 mm and RMSE under 0.7 mm. The model accuracy was lower in the case of three rainfall events (20%), namely those on 7 June 2018, 6 September 2015, and 22 June 20Thetive cells), and the lowest for the 16 June 2016 event.

The validation of the model is highlighted mainly by a large number of cases compared to the total analyzed cases in which the model performed very well and at the same time by the higher validation percentage of about 78%, a percentage that places the model in the top quantum in terms of percentage validation. The presented model is validated and can be applied on surfaces with the same environmental characteristics in the conditions in which the precipitation core has a high precision and spatial accuracy compared to the analysis surface.

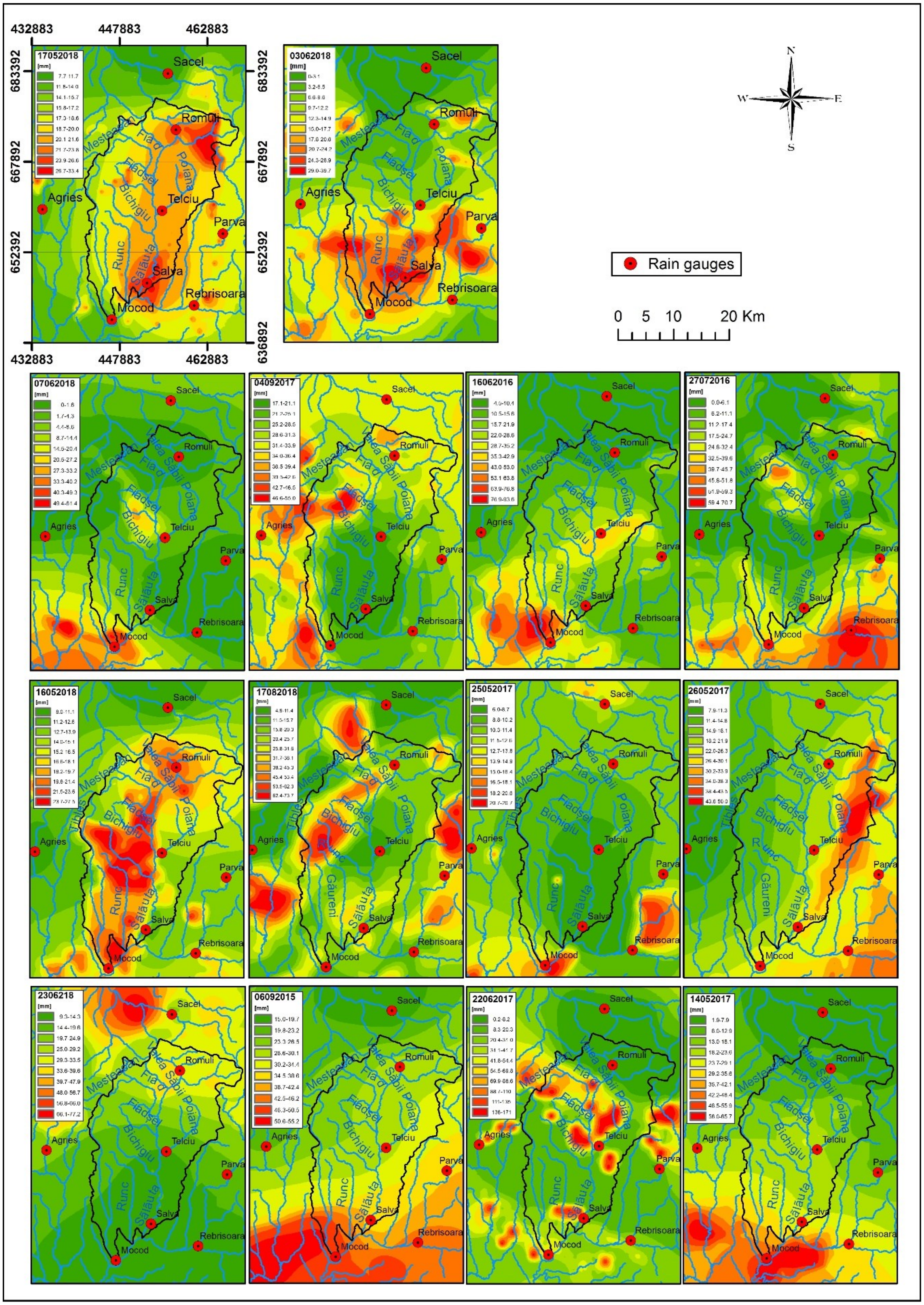

Figure 6. Merged rainfall estimates for the studied events

4.3. FREQUENCY AND INTENSITY ANALYSIS OF FLASH FLOODS

4.3.1. Results

In order to carry out the frequency analysis regarding the determination of the maximum probable discharge, generating flash floods, a number of 48 records were selected, representing the maximum discharge of flash floods, that occurred in a period of 39 years, between 1970 - 2008, at Huta Certeze h.s., from the upper part of the Valea Rea river basin *(Table 1)*.

Table 1. The maximum discharge of flash floods recorded at Huta Certeze h.s.

Q mc/s	**Date**	**Q mc/s**	**Date**
89.6	12/05/1970	16.6	29/03/2000
47.2	12/06/1974	22	06/04/2000
48.2	12/12/1979	13	06/02/2001
30.2	21/07/1980	28.4	04/03/2001
33.4	22/07/1980	12.5	18/06/2001
28.8	14/10/1980	4.81	04/07/2001
13.1	10/03/1981	16.5	18/09/2001
26.7	12/03/1981	17.2	14/11/2001
26.7	12/12/1981	13.8	30/12/2001
13.5	02/01/1982	4.1	28/01/2002
18.9	28/06/1982	6.47	01/02/2002
55.9	20/12/1993	18.6	10/02/2002
31.4	19/10/1996	28.6	03/03/2002
18.9	21/12/1996	5.63	26/10/2002
25.2	29/10/1998	10.6	29/12/2002
33.5	30/10/1998	21.1	31/12/2002
23.3	04/11/1998	18.1	25/03/2004
9.15	12/01/1999	12.8	20/04/2005
13.7	07/03/1999	24.8	21/04/2005
5.17	10/03/1999	15	28/04/2005
15.2	12/03/1999	15	09/08/2005
12.5	19/04/1999	36.6	25/08/2005
15.4	09/02/2000	19.5	29/04/2006
15.4	09/03/2000	12.8	13/04/2008

The frequency analysis on the data set regarding the determination of the discharges corresponding to the exceedance probabilities of 0.1%, 0.5%, 1%, 2%, 5%, and 10% was carried out with the *HyfranPlus* program; being designed to calculate the exceedance and non-exceedance probabilities of some events, based on the statistical analysis of long strings of databases (Bilașco & Horváth, 2016).

The calculation of the return period and the probability analysis were performed by selecting the *Pearson type 3* function *(Figure 7),* a function used with good results both internationally (Cooper, 2005), and for the territory of Romania (Bilașco, 2009).

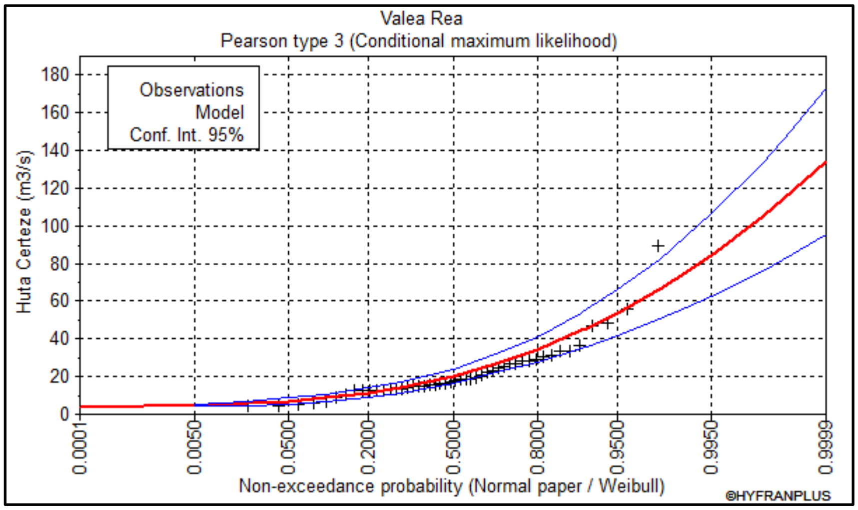

Figure 7. Graphic representation of flood discharges from Huta Certeze h.s., with Pearson Type 3 function

t On August 1, 2019, at Huta Certeze h.s. following a prefrontal convective rain, 132.5 l/m^2 were recorded, generating a flash flood, with a peak discharge of 46.6 m^3/s. Thus, in order to validate the results of analyzing the frequency of flash floods, we introduced the intermediate probability of 11 years, representing the years between the final date of the data set and the year of occurrence of the flood mentioned above. Thus, the probable discharge result with a return period of 11 years is 45.8 m^3/s, with a non-exceeding probability of 0.909 which falls within the confidence interval, 95% confidence level, in the range of 36.0 – 55.5 *(Table 2)*.

Table 1. Results obtained after applying the frequency analysis function (Pearson Type 3)

Nr.	Time (T) years	Probability of non-exceeding (q)	Probable discharge value (Q) mc/s	Standard deviation	Confidence interval 95%
1	1000	0.999	105	14.7	76.2 - 134
2	200	0.995	84.4	11.1	62.5 - 106
3	100	0.990	75.4	9.63	56.5 - 94.3
4	50	0.980	66.3	8.15	50.3 - 82.2

5	20	0.950	54.0	6.21	41.8 - 66.2
6	11	0.909	45.8	4.98	36.0 - 55.5
7	10	0.900	44.4	4.79	35.1 - 53.8

5. GIS MODEL FOR DIGITAL MAPPING OF THE AREAS VULNERABLE TO FLASH FLOODS

By using GIS methodologies, which involve the integration of spatial databases, the areas vulnerable to flash floods were mapped, respectively with the SCS-CN method were highlighted the effects that the intensification of land use has on surface runoff within the studied hydrographic basins.

5.1. REALIZATION THE FLOOD SUSCEPTIBILITY MAP, BY APPLYING THE WofE BIVARIATE STATISTICAL ANALYSIS MODEL. APPLICATION IN THE VALEA REA HYDROGRAPHIC BASIN

In order to create the flood susceptibility map, the Valea Rea hydrographic basin was selected, as being an area susceptible to the occurrence of flash floods, because it is exposed to the western circulation, which favours the development of such processes. The entire research is based on a methodology involving the integration of spatial databases, which indicate the vulnerability of the territory in the form of a weighted average equation to highlight the major impact of the most relevant factor (Kocsis et al., 2022).

5.1.1. Methodology and databases

The high complexity of the spatial analysis model presented in this research supposes the approach of a methodology that allows for the management of spatial and alphanumeric databases in such a way as to highlight the local and general specificity of each database which makes up the final model (Kocsis et al., 2022). The analysis of each component and their integration in the form of spatial analysis equations based on mathematical equations and weighted averages finalises the model and allows the spatial identification of areas that have different types of vulnerabilities to flash floods.

The proposed methodology is structured into four main stages, starting from the database acquisition, then the performance of the detailed spatial analysis, the presentation of the final results, and the validation of the results for the proposed model in order to be scientifically applied in practice *(Figure 8)*.

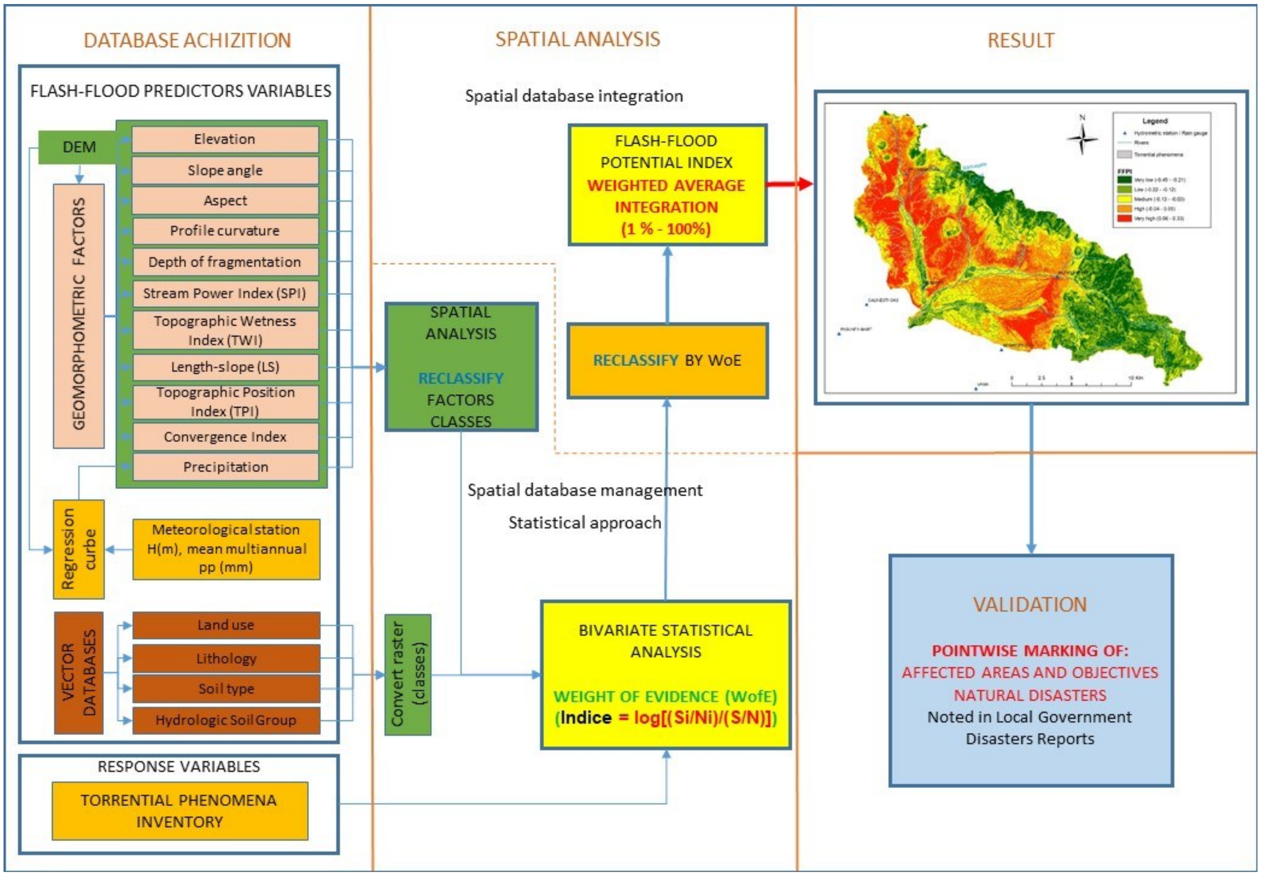

Figure 83. Flowchart of the methodology

The high complexity of the spatial databases which make up the proposed model determines the identification of two distinctive substages, embodied in one substage of spatial analysis, and the other substage integrates a distinctive spatial analysis submodel to spatialise the multiannual average amount of precipitation.

The spatial analysis submodel proposed for the spatialisation of the average amount of precipitation according to altitude is based on the statistical spatial analysis implemented according to spatial analysis equations obtained as a result of the identification of the regression line and its equation. Therefore, the following equation has been used for the entire study area *(1)*:

$$Y = a + b \ln(x) \qquad (1)$$

where: a = -148.377; b = 190.707; x = altitude

The equation was obtained by implementing the precipitation and altitude values for a number of nine stations unevenly distributed across the study area and its immediate vicinity, using Curveexpert software. A correlation coefficient of 0.980 was obtained, providing a 95% confidence coefficient.

The spatial analysis stage is the main and fundamental stage for finalising the proposed model to identify vulnerable areas. The development of the main stage of spatial analysis is based on the implementation of two spatial analysis submodels that are different in terms of the manner of implementation. They are developed according to spatial analysis equations derived from different equations in terms of structuring manner, as one model is based on a bivariate statistical equation and the other model is based on a deterministic equation that integrates the spatial databases resulting from the implementation of the first model.

The model based on statistical analysis is centred on the bivariate equation *WofE (2)* and allows the analysis of the basic components of the model to identify the behaviour of each analysed factor concerning the statistical answer to flash flood occurrence.

$$(Index = log[(Si/Ni)/(S/N)]) \qquad (2)$$

where:

- Index = the statistical value of the interval within the analysed factor
- Si = the area (sq km) with torrents on an interval of the analysed factor
- Ni = the total area covered by the analysed factor (sq km)
- S = the total area with torrents within the entire study area (sq km)

The finalisation of the spatial analysis submodel involves several main substages that are highly correlated to each other and converge to the acquisition of numeric databases which are integrated into a statistical formula, highlighting the statistical behaviour of each interval of the analysed factor.

One main stage is represented by the uniformisation of the types of databases that enter the spatial analysis model. The resolution of the raster databases acquired as a result of conversion is three, which is equal to the one of the spatial databases derived from DEM.

The second stage of the submodel is represented by the spatial integration of the analysed factors with the areas covered by torrents in order to extract numerical values for areas, to be introduced in the statistical equation for computing. This stage has in its centre the overlay vector–raster analysis, integrating, on one hand, the vector databases representing the spatial extension of the torrents, and on the other hand, the raster databases representing each factor classified according to its susceptibility to flash floods.

The second main submodel of the spatial analysis stage proposes the integration of all the factors unitarily analysed within the statistical submodel based on the WofE equation according to a deterministic spatial analysis equation of the weighted average type.

The integration of the two submodels in the spatial analysis stage is made according to the reclassification method, the main purpose of which is the acquisition of digital data in a raster format to highlight spatially the numeric values of every factor and its degree of susceptibility to flash floods and to allow their integration based on the deterministic equation. The deterministic equation *(3)* was implemented in the GIS environment in the following form:

*("BSA_SPI.tif" * 2) + ("BSA_LS.tif" * 8) + ("BSA_PP.tif" * 7) + ("BSA_DepFrag_ha.tif" * 8) + ("BSA_TPIndex3.tif" * 5) + ("BSA_DEM.tif" * 2) + ("BSA_Convergente_Index.tif" * 7) + ("BSA_Profile_curv.tif" * 8) + ("BSA_Aspect.tif" * 3) + ("BSA_Slope.tif" * 15) + ("BSA_HSG_cor.tif" * 10) + ("BSA_Lithology_cor.tif" * 2) + ("BSA_CLC.tif" * 10) + ("BSA_SOL_Tip.tif" * 5) + ("BSA_TWI.tif" * 8)/15 (3)*

where:

- "BSA_SPI.tif"…= analysed factor
- 2…= percentage weighting the factor
- +,/,* = mathematical identifiers

The specific weight of each factor was established according to the importance and influence of the factor within the general process related to the emergence and development of flash floods.

5.1.2. Results

The territorial specificity from the point of view of the FFPI is given by the statistically-based integrated analysis of a number of 15 factors that best highlight the territorial development of the analysed process *(Table 3, 4; Figures 9, 10, 11, 12)*.

Table 3. Flash flood predictor variables classes with their WofE results (Kocsis et al., 2022)

Predictors Variables	Class	Pp (%)	Pt (%)	WofE	WAI (%)
Elevation	145 - 300	42.6	82.3	0.29	2
	300 - 450	24.5	15.2	-0.21	
	450 - 650	17.9	2.4	-0.87	
	650 - 850	10.2	0.2	-1.80	
	850 - 1239	4.7	0.0	-	
Slope angle	0-3	22.0	17.2	-0.11	15
	3.1-7	19.8	34.1	0.24	
	7.1-15	32.6	35.6	0.04	
	15.1-25	17.1	10.5	-0.21	
	> 25	8.5	2.6	-0.51	
Aspect	Flat/Southwest	17.0	9.4	-0.26	3
	South	13.0	10.7	-0.09	
	Southeast/West	28.7	26.4	-0.04	
	East/Nortwest	24.1	24.3	0.00	
	North/Northeast	17.3	29.3	0.23	
Profile curvature	Convex-209 - 0	50.6	33.9	-0.17	8
	Flat 0 - 1.92	47.2	55.6	0.07	
	Concave 1.92 - 199	2.2	10.5	0.69	
Depth of fragmentation	0-2	27.5	22.0	-0.10	8
	2-4	35.1	52.7	0.18	
	4-8	20.3	17.9	-0.05	
	8-16	11.8	6.4	-0.26	
	16-110	5.3	1.0	-0.73	
SPI	(-13.8) - (-11.3)	5.6	4.4	-0.10	2
	(-11.2) - (-4.33)	22.0	17.0	-0.11	
	(-4.32) - (-2.55)	39.3	38.5	-0.01	
	-2.54 - 0.52	31.1	31.4	0.00	
	0.53 - 11.4	2.1	8.7	0.62	
TWI	0-2.49	6.6	4.7	-0.14	8
	2.50-6.04	25.8	19.5	-0.12	
	6.05-8.06	44.1	40.5	-0.04	
	8.07-11.6	21.3	26.7	0.10	
	11.7-30.2	2.2	8.5	0.59	
L-S Factor	0-2	67.1	62.5	-0.03	8
	2-6	23.1	20.4	-0.06	
	6-10	5.9	6.4	0.04	
	10-50	3.7	10.3	0.45	
	50-190	0.1	0.3	0.41	
TPI	(-35.3) - (-7.10)	3.5	18.3	0.73	5
	(-7.09) - (-2.1)	16.5	52.5	0.50	

	(-2.09) - 1.66	57.3	28.8	-0.30	
	1.67- 6.98	18.6	0.4	-1.68	
	6.99 - 44.5	4.2	0.0	-	

Pp (%) - percentage of class pixels; Pt (%) - percentage of torrential pixels; WAI - Weighted Average Integration

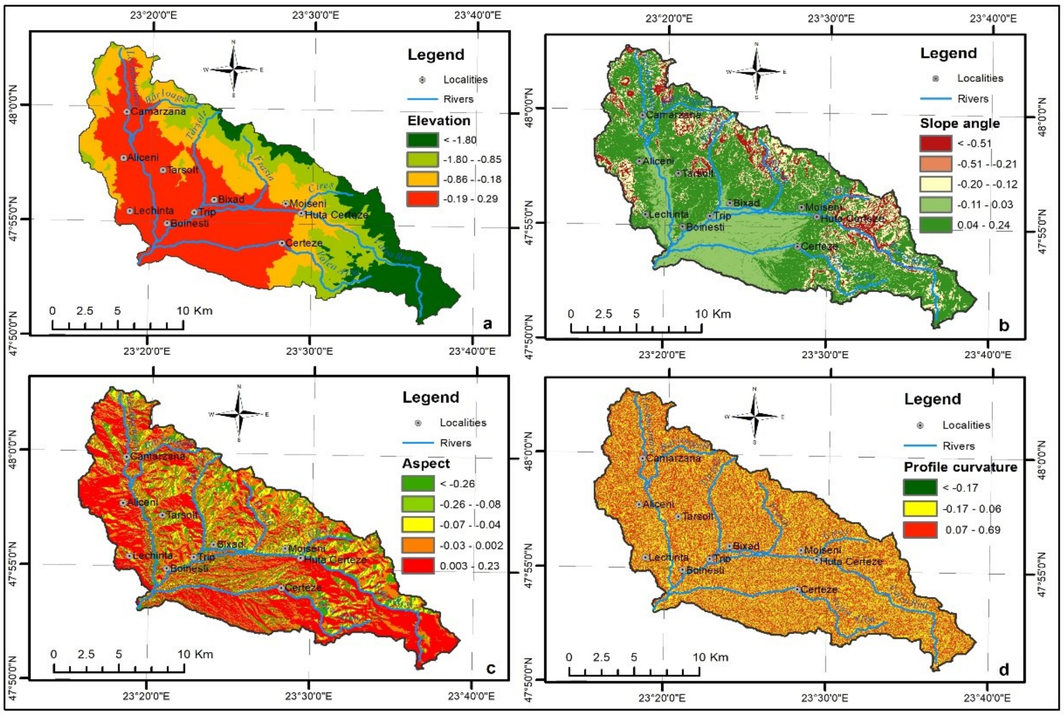

Figure 9. Valea Rea catchment basin: a) elevation, b) slope angle, c) aspect,

d) profile curvature.

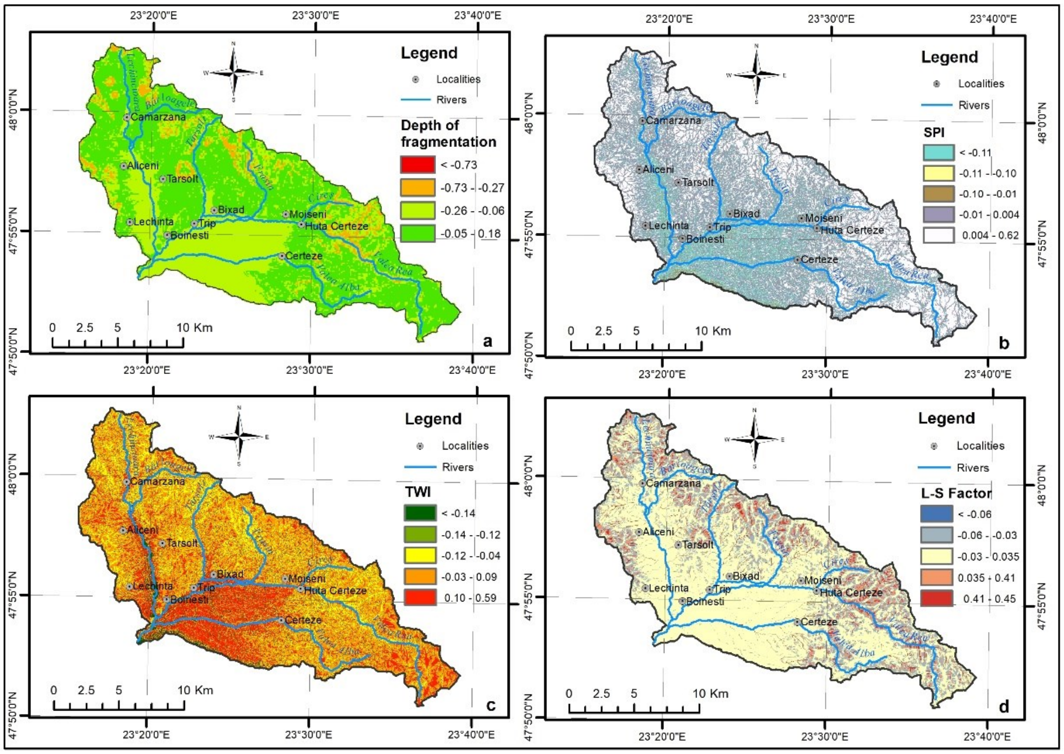

Figure 10. Valea Rea catchment basin: a) depth of fragmentation, b) SPI, c) TWI, d) L-S factor

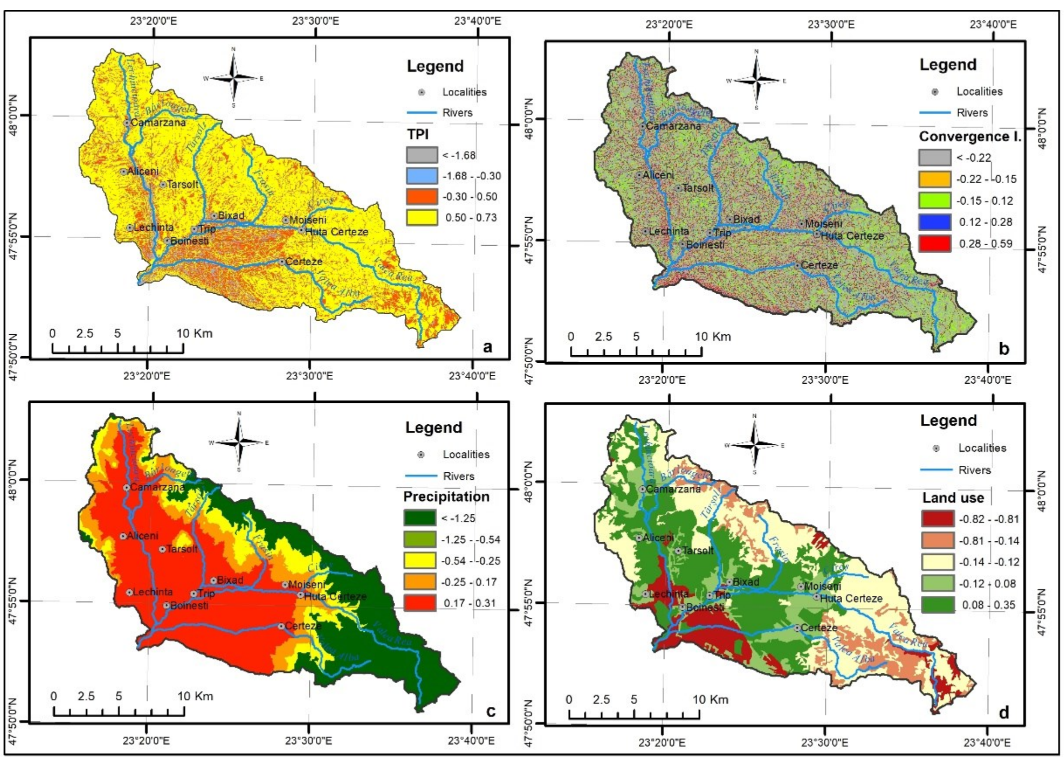

Figure 11. Valea Rea catchment basin: a) TPI, b) convergence index, c) precipitation, d) land use

Table 4. Flash flood predictor variables classes with their WofE results (Kocsis et al., 2022)

Predictors Variables	Class	Pp (%)	Pt (%)	WofE	WAI (%)
Convergence Index	0.1 - 99	53.3	31.9	-0.22	7
	(-0.9) - 0	26.6	19.0	-0.15	
	(-1.9) - (-1)	8.3	11.0	0.13	
	(-2.9) - (-2)	3.8	7.3	0.28	
	(-99) - (-3)	7.9	30.8	0.59	
Precipitation	800-850	14.3	21.2	0.17	7
	850-950	32.0	65.8	0.31	
	950-1000	13.6	7.6	-0.25	
	1000-1050	13.1	3.8	-0.54	
	1050-1209	27.1	1.5	-1.25	
Land use	Discontinuous urban fabric	5.7	4.8	-0.12	10
	Non-irrigated arable land	8.0	0.0	-	
	Fruit trees and berry plantations	13.6	26.7	0.25	
	Pastures	14.7	19.6	0.08	
	Complex cultivation patterns	7.2	9.2	0.06	
	Land principally occupied by agriculture, with significant areas of natural vegetation	3.6	9.0	0.35	
	Broad-leaved forest	35.8	29.2	-0.13	
	Coniferous forest	0.3	0.0	-	
	Mixed forest	1.3	0.0	-	
	Natural grasslands	9.3	1.6	-0.82	
	Transitional woodland-shrub	0.5	0.0	-	
	Sparsely vegetated areas	0.1	0.0	-	
Lithology	Amphibole andesites	0.1	0.0	-	2
	Basaltic andesites	36.2	20.1	-0.17	
	Quartz andesites	5.8	2.6	-0.35	
	Pyroclastic rocks	4.3	4.4	0.01	
	Argillaceous marls/marlstones, sand, gravel	23.6	32.6	0.14	
	Andesites	0.6	1.2	0.27	
	Alluvial deposites, proluvium	3.2	14.8	0.67	
	Porphyry granodiorites	0.6	0.9	0.19	
	Diluvium	11.1	0.1	-2.10	
	Gravel, sand, and argillaceous sand	13.4	19.2	0.16	
	Porphyry diorite	1.0	4.1	0.59	
Soil type	Acid brown soils	22.4	7.1	-0.50	5
	Brown luvic (podzolic) soils	21.8	42.3	0.29	
	Clayish brown luvisols	15.0	22.9	0.18	
	Lithosols	3.4	2.6	-0.12	
	Albeluvisols (podzoluvisols)	18.5	23.1	0.10	
	Eu-mesobasic brown soils	9.2	2.0	-0.70	
	Andosols	9.7	0.0	-	
	Alluvial soils	0.0	0.0	-	

HSG	D	46.9	22.3	-0.32	10
	B	41.7	71.3	0.23	
	C	11.4	6.4	-0.25	

Pp (%) - percentage of class pixels; Pt (%) - percentage of torrential pixels; WAI - Weighted Average Integration

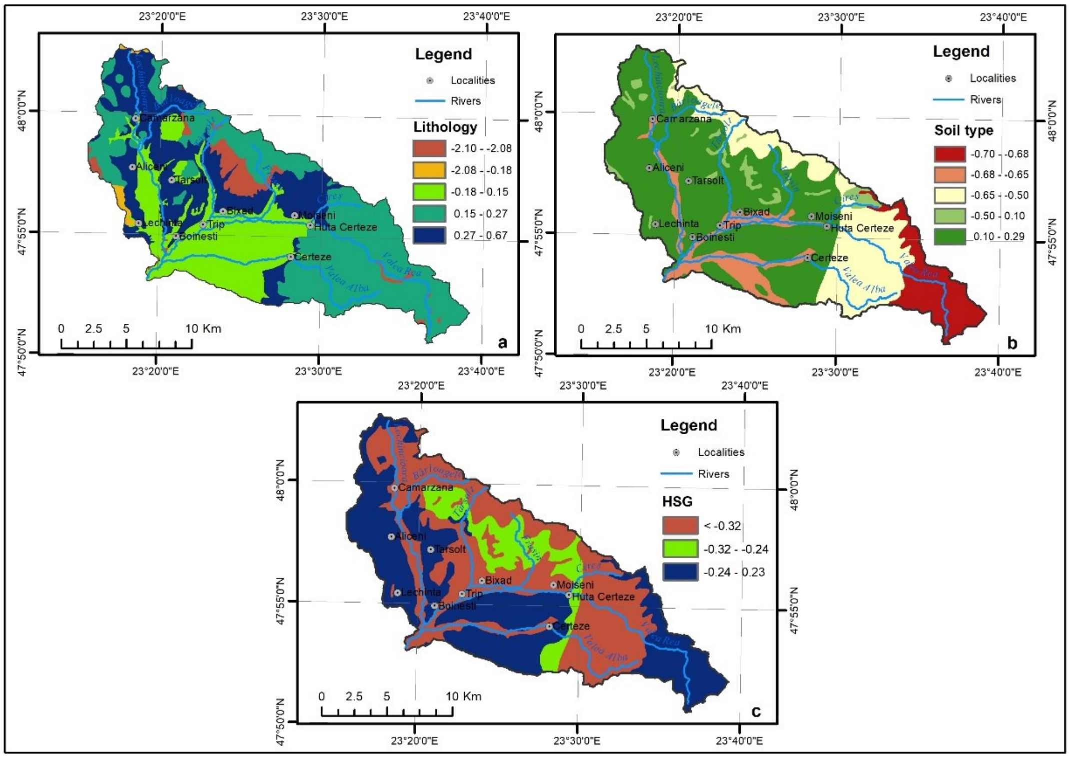

Figure 12. Valea Rea catchment basin: a) lithology, b) soil type, c) HSG

$FFPI_{WofE}$ Distribution in the Valea Rea River Catchment

The integration of the unitary analysed factors for the acquisition of the final databases, representative for the analysed territory from the FFPI perspective, has been carried out according to the *"weighted average overlay"* method. The result was a spatial database, classified into five classes (from very low to very high), representing the territorial vulnerability in terms of FFPI *(Figura 13)*.

Analysing the results obtained as a consequence of the implementation of the spatial analysis model on three vulnerability classes: low (low and very low vulnerability), medium (spatially covering the transition area), and high (high and very high vulnerability), the high vulnerability of the study area in terms of FFPI is clearly emphasised because this class spatially covers approximately 43% of the analysed study area.

At the level of the territory, there is a major impact due to the fact that the entire class of high vulnerability covers the built-up areas of the villages within the analysed region and is also manifest in the areas with the highest density of residential households and their associated infrastructure.

The validation of the spatial analysis model was performed by directly comparing the obtained results with places where flash floods occurred, randomly identified in the study area. Therefore for validation, two sites have been selected in order to cover as much of the analysed area as possible.

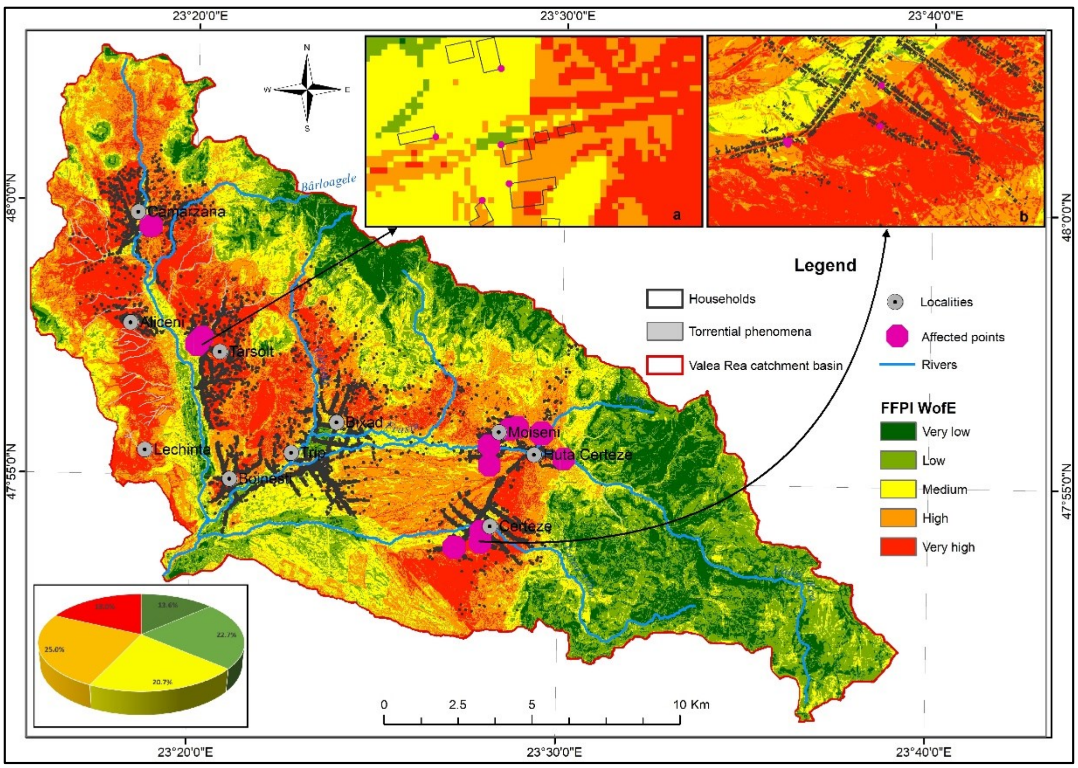

Figure 13. Valea Rea catchment basin: $FFPI_{WofE}$ distribution, a) validation area 1, b) validation area 2.

5.2. LAND USE AND ITS IMPORTANCE IN FLOOD ESTIMATION MODELS. APPLICATION IN THE ȚIBLEȘ-RUNC-SĂLĂUȚA HYDROGRAPHIC BASIN

5.2.1. Methodology and databases

The study carried out on the neighbouring Țibleș, Runc and Sălăuța watersheds aims to investigate the land use/land cover changes over time, and their impact on surface runoff, based on the SCS-CN method in the GIS environment. For this purpose, the study uses the Corine Land

Cover (CLC) databases from the years 2000, 2006 and 2012, respectively the GIS extension ArcHydro for the watersheds delineation and the analysis of the study area. Changes in the field are analyzed comparatively both at a relatively short level in terms of duration and a long level (taking into account the changes produced during the whole time period), to observe whether or not their rate intensifies with the passage of time.

A second analysis refers to the contribution of each type of use according to different scenarios of antecedent moisture condition (AMC), to the same rainfall event, taking into account both the total runoff volume at the catchment closure points and its spatial distribution at the pixel level and usage category.

In a later step, the CN Index was adjusted according to different scenarios of antecedent soil moisture conditions.

5.2.2. Results

As regards the land use structure between 2000 and 2012, the watersheds share the same pattern of land use change. There was a loss in forest cover and pastures due to agricultural expansion.

Overall, the highest changes occurred between 2000 and 2006 with the conversion of forest land to agricultural use (occupying 6,8% and 4,4% more of the total areas of Țibleș and Sălăuța, respectively).

Therefore, considering the entire study area, the base year of 2000 and the micro-scale classification of land uses, the complex cultivation, orchard, natural grassland, moor, and heathland areas experienced the most notable changes that took place during the first seven years of the studied period. The natural grassland areas had nearly doubled in size, leading to the disappearance of moors and heathlands, and the complex cultivation areas have increased by over 50%. The orchards had the highest increase in area, although in 2000 they occupied just 1 km^2 of the total Țibleș river catchment area.

As mentioned above, the SCS-CN method was used for surface runoff simulation, the other key factors being considered constant, in order to accurately evaluate the land use-runoff relationship. The method was implemented in a GIS environment and the spatial statistics and analysis functions were used to compute the values. Considering the maximum runoff volume per pixel, the results revealed no significant difference between the time periods under the same AMC scenario. *(Table 5)*.

Table 5. Estimated runoff volumes at cell (pixel) level

Watersheds	AMC classes	Runoff volume (m^3/cell)								
		2000			2006			2012		
		Min.	Med.	Max.	Min.	Med.	Max.	Min.	Med.	Max.
TIBLEȘ	AMC1	0.000	1.52	13.8	0.000	1.70	13.8	0.000	1.71	13.8
	AMC2	0.040	4.63	18.8	0.040	4.87	18.8	0.110	4.90	18.8
	AMC3	2.07	8.74	23.2	2.06	8.96	23.2	2.60	8.99	23.1
RUNC	AMC1	0.000	1.80	8.50	0.000	1.90	8.50	0.000	2.0	8.60
	AMC2	0.000	5.30	14.7	0.000	5.40	14.7	1.00	5.50	14.9
	AMC3	2.00	9.60	18.9	2.00	9.70	18.9	4.00	9.80	19.1
SĂLĂUȚA	AMC1	0.000	0.800	11.2	0.000	0.900	11.2	0.000	0.900	12.0
	AMC2	0.000	3.30	15.5	0.000	3.40	15.5	0.000	3.40	16.6
	AMC3	0.100	6.80	17.9	0.100	6.90	17.9	0.100	6.90	19.0

Based on the spatial distribution of the runoff volumes, regardless of the antecedent moisture conditions, the largest changes can be observed in the middle and downstream catchments of the main rivers where agricultural activities are the most intense and the few forested areas existent here, actually shrunk over time. According to the chosen rainfall event scenario, notable differences in each catchment area's total runoff volume have been observed over time *(Table 6)*.

Table 62. The total estimated runoff volume

Watersheds	AMC classes	Total runoff volume (m^3)		
		2000	2006	2012
TIBLEȘ	AMC1	240440	268311	270517
	AMC2	732517	770718	774670
	AMC3	1381816	1416492	1421849
RUNC	AMC1	141369	150738	157419
	AMC2	412915	422658	427118
	AMC3	750266	759371	762513
SĂLĂUȚA	AMC1	545683	577335	585489
	AMC2	2172470	2218413	2233001
	AMC3	4510732	4560759	4577983

By analyzing these changes as a percentage of the base values (from the beginning of each study time period), the same pattern could be observed for all of the catchment areas, with greater changes between 2000 and 2006, strongly linked to the changes in vegetation.

6. VALIDATION OF THE GIS MODEL BASED ON THE CASE STUDY METHOD: THE FLASH FLOOD OF AUGUST 1, 2019 OCCURRED IN THE UPPER VALEA REA RIVER BASIN

The flash flood that occurred on August 1, 2019, at Huta Certeze hydrometric station, was chosen for the physical validation of the "GIS model for digital mapping of the areas vulnerable to flash floods".

The total amount of accumulated water, measured at Huta Certeze hydrometric station was 132.5 l/m^2. The maximum level observed at Huta Certeze h.s. was 225 cm from the "0 staff" level, exceeding the Flood Level by 25 cm. Starting from the base flow of 0.265 m^3/s, observed on the morning of the event at 06:00, the maximum discharge recorded was 46.6 m^3/s, which occurred at 17:30, thus forming a single-wave flood.

6.1. Methodology

For modeling the flash flood that occurred on the 1st of August 2019, I used the *Mike Hydro River* program, a hydrological model that uses the *Unit Hydrograph Method (UHM)* from the *Rainfall-Runoff Module,* in order to obtain the runoff hydrograph recorded at the hydrometric station.

Therefore, four different options are available to represent the loss model (Strapazan et al., 2021), each requiring different inputs: *Constant loss, Proportional loss*, *SCS Method,* and *SCS generalised.*

6.2. Results

The flash flood simulation was performed with MIKE HYDRO River -UHM, using as input data the precipitation measured at Huta Certeze h.s. All four methods were used to calculate infiltration losses. *(Table 7, Figure 15).*

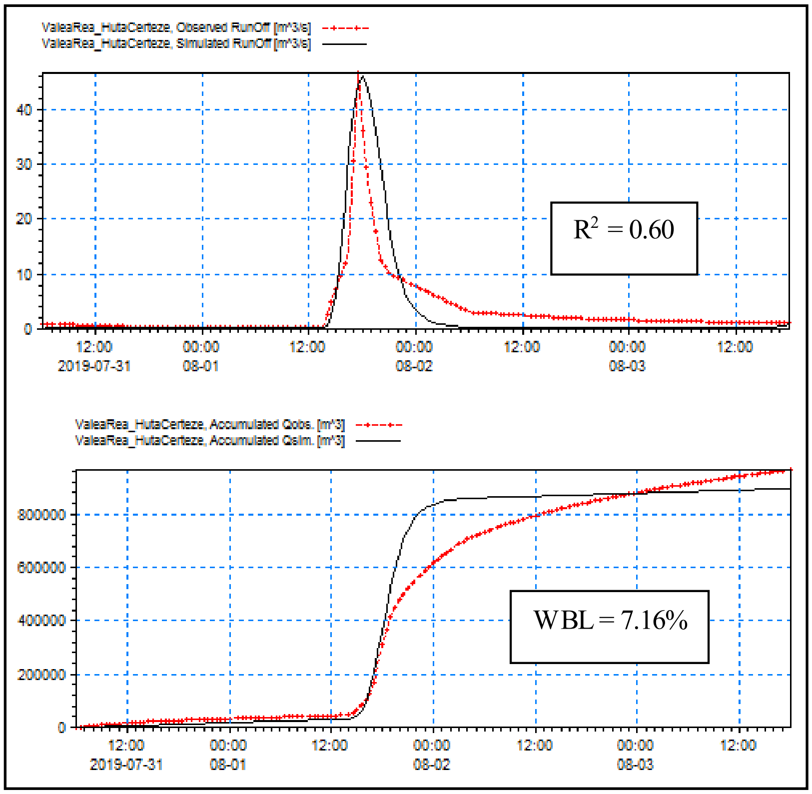

Figure 14. UHM auto-calibration, Proportional loss method

The discharge hydrograph simulated with the *Proportional Loss* method reproduces the most credible the breakout moment and propagation of the flash flood, compared to the observed hydrograph characteristics, being authenticated by the auto-calibration results used by MIKE: $R^2 = 0.60$, water balance (WBL) = 7.16% *(Figure 14)*.

Table 7. Simulation results

Infiltration Losses Model Type	Parameters	Accumulated Volume [m^3]	Maximum simulated discharge [m^3/s]	Errors compared to the maximum discharge recorded	
				amplitude	phase
Constant Loss	Initial loss: 48 mm Constant loss: 30 mm/h Lag time: 2.53 Area adjustment factor: 1	736755.40	48.5	+ 4.1 %	+ 30 min
Proportional Loss	Runoff coefficient: 0.1 Lag time: 2.53 Area adjustment factor: 1	896280.71	46.1	- 1%	+ 30 min
SCS method	CN = 63 Initial AMC = 1 Lag time: 2.53 Area adjustment factor: 1	728506.90	44.1	- 5.4%	+ 2 h
SCS generalised	CN = 63 Initial abstraction depth: 87 Lag time: 2.53 Area adjustment factor: 1	745127.34	46.9	+ 0.6%	+ 2 h

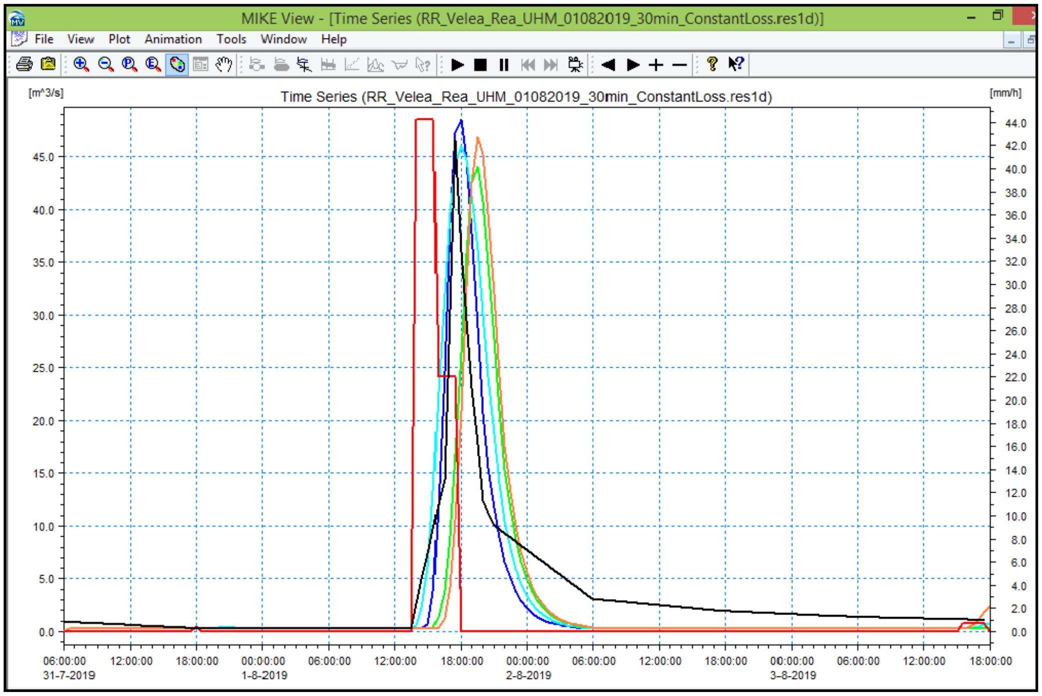

Figure 15. Discharge hidrograph (__ recorded, __ Constant Loss, __ Proportional Loss, __ SCS method, __ SCS generalised, __ Observed precipitation)

7. CONCLUSIONS

Following the study carried out regarding the *"Determination of the precipitation potential of cloud forms based on radar images"*, we can state that in the case of convective and prefrontal situations, the RDOD and RDBB radars capture the areas with precipitation together with their quantitative peaks, also showing significant differences in the peripheral regions of the study area.

In the case of frontal situations, when the fronts appear in the morning hours, the meteorological radar does not estimate the amounts of cumulative precipitation, with the mention that the RDBB observes the areas with quantitatively significant precipitation, but with imprecise estimates.

In the study of *"correction of radar-estimated precipitation amounts based on in situ measurements for precipitation spatialisation"*, reliable merged precipitation maps from two different sources of databases were obtained for 15 rainfall events, produced in the Țibleș, Runc and Sălăuța river basins.

An important outcome of this study was the validation of the CMT method, to be used within the hydrographic studied basins. In conclusion, we noted that the accuracy of the model was lower in the case of high-intensity, local torrential (convective cells) rainfall events, where extreme values and consequently large variability of the measured values were detected, and with high accuracy in the case of evenly distributed rainfall events (frontal systems). Overall, the final model performed well in estimating the spatial distribution of different rainfall events (Kocsis et al., 2022).

The CMT methodology used provides a potential advantage for extending radar–rain gauge merged precipitation to those small-size watersheds where gauge observation is limited or completely missing.

Elaboration of the study *"realization the flood susceptibility map, by applying the WofE bivariate statistical analysis model",* within the Valea Rea h.b. represented the main objective of the research thesis. The structure of the presented model fits the general methodologies based on the statistical analysis to identify the territorial vulnerability to slope flash floods, implementing a number of new factors (depth of fragmentation, soil type, precipitation) which influence their development and propagation. Taking into account the mechanisms governing the development of flash floods and based on expert knowledge analysis, it was decided to assign the highest weight to the slope factor, followed by LULC and HSG. The factors that have the lowest weight are represented by lithology, SPI, and elevation, which do not have a direct influence on runoff (Kocsis et al., 2022).

The model was validated by directly comparing the results obtained with locations previously affected, where the flood effects have been identified, highlighting the fact that the model may be taken into account to be applied in practice, and also to be implemented in territories that share the same features.

The presented methodology was applied to identify the areas prone to flash floods in different degrees, from very low to very high vulnerability. It also highlights that areas with high and very high vulnerability cover approximately 43% of the total catchment, highlighting the excessively torrential nature of the study area and the potential risks for the territorial infrastructure.

The study on "*land use and its importance in flood estimation models*" represents another model, different from the previous one, that can be successfully implemented to identify areas vulnerable to flash floods.

Simulation of the rainfall-runoff process, based on a large and uniformly distributed rainfall event, concerning historical land use changes and different antecedent moisture conditions, demonstrated that basins and related runoff volumes are highly sensitive to agricultural activities. The study carried out showed that even the smallest changes leave their mark on the runoff within mountain basins with different surfaces. The only advantage is the fact that in the last half of the analyzed period, the vegetation has not undergone such large changes, which leads to a certain decrease in agricultural practices and a decrease in the runoff potential.

In conclusion, if this trend continues, it could lead to stagnant agricultural exploitation and reduced runoff potential.

The case study: The flash flood of August 1, 2019, occurred in the upper Valea Rea river basin, at Huta Certeze h.s., was chosen in order to physically validate the GIS model for mapping areas vulnerable to flash flood.

The deviations obtained compared to the maximum recorded discharge have an amplitude between -5.4% and +4.1%, with a gap regarding reaching the peak discharge of +30 min. and 2 h, in the case of the two SCS methods.

The good results obtained with all four methods confirm that MIKE HYDRO River - UHM can be used for forecasting water flows to rivers or lakes, estimating water resources, managing flood risk, as well as to physically validating studies on creating susceptibility and vulnerability maps to floods in torrential watersheds.

In addition to the physical validation, the GIS spatial analysis model proposed for the "*digital mapping of the areas vulnerable to flash floods within torrential basins"*, was also subjected to statistical validation. As a result, a frequency model validated both statistically and physically can be used in speciality practice.

Risk assessment is a necessary stage in the process of integrated territorial management to highlight viable areas for the development of human activities. The proposed spatial analysis GIS model for *digital mapping of the areas vulnerable to flash floods within torrential basins* may represent a methodology to be applied in spatial planning studies, highly useful in land management and for local governments in mitigating the risk of flash floods. Future studies regarding the analysed area will focus on risk assessment concerning all territorial infrastructures and the solutions meant to mitigate these risks.

8. SELECTIVE BIBLIOGRAPHY

1. Aquaproiect S.A. (2014). *Planul pentru prevenirea, protecția și diminuarea efectelor inundațiilor (PPPDEI) în bazinul hidrografic Someș Tisa.*
2. Armas, I. (2012). Weights of evidence method for landslide susceptibility mapping. Prahova Subcarpathians, Romania. *Journal of Natural Hazards, 60*(3). https://doi.10.1007/s11069-011-9879-4
3. Barredo, J. I., Roo, A., & Lavalle, C. (2007). Flood risk mapping at European scale. *Journal of water science and technology, 56,* 7-11. https://doi.10.2166/wst.2007.531
4. Bilașco, Ș. (2008). *Implementarea G.I.S. în modelarea viiturilor de versant*. Casa Cărții de Știință, Cluj-Napoca.
5. Bilașco, Ș., & Horváth, Cs. (2016). *Cartografierea digitală a benzilor de inundabilitate pe baza statisticii, a calculelor hidraulice și a analizei spațiale GIS.* Casa Cărții de Știință, Cluj-Napoca.
6. Bilașco, Ș., Horváth, Cs., Cocean, P., Sorocovschi, V., & Oncu, M. (2009). Implementation of the USLE model using GIS techniques. Case study The Someșean Plateau. *Carpathian Journal of Earth and Environmental Sciences, 4*(2), 123-132.
7. Bilasco, S., Horvath, Cs., Roșia, G., Filip, S., & Keller, I. E. (2011). Statistical model using GIS for assessment of landslide susceptibility. Case-study: The Someș Plateau. *Rom J Geogr, 55*(2), 91-111.
8. Blöschl, G., & Grayson, R. (2001). Toward Capturing Hydrologically Significant Connectivity in Spatial Patterns. *Water Resources Research, 37*(1), 83-98. https://doi.10.1029/2000WR900241
9. Braxton, E. (2006). GIS-based radar rainfall verification. *Significant Opportunities in Atmospheric Research and Science.* USA.
10. Brewster, J. (2009). *Development of the Flash Flood Potential Index.* http://www.erh.noaa.gov/bgm/research/ERFFW/presentations/june02_2010/Brewster_Jim_Development_of_FFPI.ppt. (accessed on 9 February 2022).
11. Burcea, S., Cheval, S., Dumitrescu, A., Antonescu, B., Bell, A., & Breza, T. (2012). Comparison between radar-estimated and rain gauge-measured precipitation in the Moldovan Plateau. *Environmental Engineering and Management Journal, 11*(4), 723-731. https://doi.10.30638/eemj.2012.093
12. Castellarin, A., Kohnová, S., Gaál, L., Fleig, A., Salinas, J. L., Toumazis, A., Kjeldsen, T. R., & Macdonald, N. (2012). *Review of applied-statistical methods for flood-frequency analysis in Europe.* Technical report (NERC) Centre for Ecology & Hydrology.
13. Chendeș, V. (2011). *Resursele de apă din Subcarpații de la Curbură. Evaluări geospațiale.* Editura Academiei Române, București.
14. Chiang, Y.-M., Hsu, K., Chang, F.-J., & Hong, Y. (2007). Merging multiple precipitation sources for flash flood forecasting. *Journal of Hydrology, 340,* 183-196. https://doi.10.1016/j.jhydrol.2007.04.007
15. Costache, R., & Zaharia, L. (2017). Flash-flood potential assessment and mapping by integrating the weights-of-evidence and frequency ratio statistical methods in GIS environment – case study: Bâsca Chiojdului River. *Journal of Earth System Science, 126*(4). https://doi.10.1007/s12040-017-0828-9

16. Costache, R., Hong, H., & Pham, Q. (2020). Comparative assessment of the flash-flood potential within small mountain catchments using bivariate statistics and their novel hybrid integration with machine learning models. *Science of The Total Environment, 711.* https://doi.10.1016/j.scitotenv.2019.134514
17. Costache, R., Prăvălie, R., Mitof, I., & Popescu, N.-C. (2015). Flood vulnerability assessment in the low sector of Sărățel catchment. Case study: Joseni village. *Carpathian Journal of Earth and Environmental Sciences, 10*(1), 161-169.
18. Danish Hydraulic Institute, DHI. (2017). *MIKE HYDRO River, User guide.* Danish Hydraulic Institute, Denmark. https://manuals. mikepoweredbydhi. help/2017/ Water_Resources/ MIKEHydro_River_UserGuide.pdf (accessed on 28 February 2023).
19. Deyzel, I. T. H., Pegram, G. G. S., Visser, P. J. M., & Dicks, D. (2003). *Spatial interpolation and mapping of rainfall (SIMAR): Vol. 2. Radar and satellite products. Final report to the Water Research Commission.* South African Weather Service.
20. Drobot, R. (1997). *Bazele statistice ale hidrologiei.* Editura Didactică și Pedagogică București.
21. Drobot, R., & Şerban, P. (1990). *Aplicații de hidrologie și gospodărirea apelor.* H.G.A., București. *Earth and environmental sciences, 14*(2), 439-448. https://doi.10.26471/cjees/2019/014/093
22. Ehret, U. (2002). *Rainfall and flood nowcasting in small catchments using weather radar.* [Doctoral dissertation, University of Stuttgart].
23. Goovaerts, P. (1997). Geostatistics for Natural Resources Evaluation. *Technometrics, 42*. Oxford University Press.
24. Griffis, V. W., & Stedinger, J. R. (2007). The log-Pearson type III distribution and its application in flood frequency analysis. I: Distribution characteristics. *Journal of Hydrologic Engineering, 12*(5), 482-491. https://doi.org/10.1061/(ASCE)1084-0699(2007)12:5(482)
25. Gurung, P. (2016). Integration of gauge and radar rainfall to enable the best simulation of hydrological parameters. *Hydrological Science Journal, 62,* 114-123. https://doi.10.1080/02626667.2015.1117087
26. Haidu, I. (2008). GIS and frequency analysis for the identification of vulnerable areas to extreme hydrological events. *Proceedings of the Geoinformatics Forum Salzburg, (2),* 103-108.
27. Haidu, I., Crăciun, A. I., & Bilaşco, Ş. (2007). The SCS-CN model assisted by G.I.S. – alternative estimation of the hydric runoff in real-time. *Geographia Technica, 1*, 1-7.
28. Harader, E., Estupina, V. B., Ricci, S., Coustau, M., Thual, O., Piacentini, A., & Bouvier C. (2012). Correcting the radar rainfall forcing of a hydrological model with data assimilation: application to flood forecasting in the Lez catchment in Southern France. *Hydrology and Earth System Science, 16,* 4247-4264. https://doi.10.5194/hess-16-4247-2012
29. Irimuș, I. A. (2003). *Geografia fizică a României.* Casa Cărții de Știință, Cluj-Napoca.
30. Irimuș, I. A., Vescan, I. & Man, T. (2005). *Tehnici de cartografie, monitoring și analiză GIS.* Casa Cărții de Știință, Cluj-Napoca.
31. Irimuș, I. A., Rus, M.-I., Cioban, T. D., & Bilaşco, S. (2015). Quantitative Estimation of Annual Average Rate of Soil Erosion in the Almas Hydrographical Basin, Using USLE and GIS. *15th International Multidisciplinary Scientific GeoConference on Informatics, Cartography & GIS,* 1071-1079. https://doi.10.5593/sgem2015B22

32. Ivănescu, V., Mocanu, P., & Sandu, M. A. (2014). Application of a hydrodynamic Mike 11 model for Argesel River. *14th SGEM GeoConference on water resources, forest, marine and ocean ecosystems,* 65-72. https://doi.10.5593/SGEM2014/B31/S12.009
33. Karamage, F., Zhang C., Fang, X., Liu, T., Ndayisaba, F., Nahayo, L., Kayiranga, A., & Nsengiyumva, J. B. (2017). Modeling Rainfall-Runoff Response to Land Use and Land Cover Change in Rwanda (1990–2016). *Journal of Water 9*(3), 147. https://doi.10.3390/w9020147
34. Kocsis, I., Bilaşco, Ş., Irimuş, I.-A., Dohotar, V., Rusu, R., & Roşca, S. (2022). Flash flood vulnerability mapping based on FFPI using GIS spatial analysis, case study: Valea Rea Catchment Area, Romania. *Sensors, 22*(9), 3573. https://doi.10.3390/s22093573
35. Kocsis, I., Haidu, I., & Maier, N. (2020). Application of a hydrological Mike Hydro River - UHM model for river Valea Rea (Romania). Case study, flash flood event occurred on August 1st, 2019. *Air and water components of the environment conference proceedings,* 257-272. https://doi.10.24193/AWC2020_24
36. Kocsis, I., Irimuș, I.-A., Patriche, C., Bilaşco, Ş., Maier, N., Roşca, S., Petrea, D., & Bartók, B. (2022). GIS-based methodology to combine rain gauge and radar rainfall estimates of precipitation using the conditional merging technique for high-resolution quantitative precipitation forecasts in Țibleș and Rodnei Mountains. *Atmosphere, 13*(7). https://doi.10.3390/atms13071106
37. Nițioaia, A., Maier, & N., Kocsis, I. (2021). Analysis of estimated doppler radar rainfalls. Case studies for north-western Romania using two Wsr-98d doppler radars. *Air and water components of the environment conference proceedings,* 209-224. https://doi.10.24193/AWC2021_20
38. Patriche, C. V. (2009). *Metode statistice în climatologie.* Terra Nostra. Iași.
39. Patriche, C. V., Sfîcă, L., & Roşca, B. (2008). About the problem of digital precipitations mapping using (geo)statistical methods in GIS. *Geographia Technica, 1,* 82-91.
40. Pettazzi, A., & Salsón, S. (2012, Iunie 25-29). *Combining radar and rain gauge rainfall estimates using conditional merging: a case study*. ERAD - The seventh European conference on radar in meteorology and hydrology, Toulouse, France.
41. Pișota, I., & Zaharia, L. (2002). *Hydrology.* Editura Universității, București.
42. Pișotă, I., Zaharia, L., & Diaconu, D. (2010). *Hidrologie, Ediția a II-a revizuită și adăugată.* Ediția Universitară București, București.
43. Popa, M. C., Peptenatu, D., Draghici, C., & Diaconu, D. C. (2019). Flood hazard mapping using the flood and flash-flood potential index in the Buzău River catchment, Romania. *Journal of Water, 11*(10), 2116. https://doi.10.3390/w11102116
44. Popa, M. C., Simion, A., Peptenatu, D., Dima, C., Draghici, C., Florescu, M.-S., Dobrea, R. C., & Diaconu, D. C. (2020). Spatial assessment of flash-flood vulnerability in the Moldova river catchment (N Romania) using the FFPI. *Journal of Flood Risk Management, 13*(1). https://doi.10.1111/jfr3.12624
45. Rahmati, O., Pourghasemi, H., & Zeinivand, H. (2015). Flood susceptibility mapping using frequency ratio and weights-of-evidence models in the Golastan Province, Iran. *Journal of Geocarto International.*
46. Roşca, S., Petrea, D., Bilaşco, Ş., Rus, I., Irimuş, I.-A., Fodorean, I., & Vescan, I. (2014). Assessment of Flood Hazard and Risk using GIS and Historical Data. Case-Study: The Niraj River Basin (Transylvania Depression, Romania). *14th SGEM GeoConference on Informatics Geoinformatics and Remote Sensing,* 497-509. https://doi.5593/SGEM2014/B23/S11.063

47. Sabău, D. A., Șerban, G., Kocsis, I., Stroi, P., & Stroi, R. (2018). Winter Phenomena (Ice Jam) on rivers from the Romanian Upper Tisa Watershed in the 2016-2017 winter season. *Water Management and the Environment: Case Studies* (pp. 125-174). Springer International Publishing. https://doi.10.1007/978-3-319-79014-5_7
48. Serviciul Hidrometeorologic de Stat al Republicii Moldova. (2020). *Instrucțiuni metodologice. Elaborarea prognozelor meteorologice și difuzarea de avertizări în situația producerii de fenomene atmosferice periculoase.* Chișinău.
49. Shi, P. J., Yuan, Y., Zheng J., Wang, J. A., Ge, Y., & Qiu, G. Y. (2007). The effect of land use/cover change on surface runoff in Shenzhen region, China. *Catena, 69*, 31-35. https://doi.10.1016/j.catena.2006.04.015
50. Sinclair, S., & Pegram, G. (2005). Combining radar and rain gauge rainfall estimates using conditional merging. *Atmospheric Science Letters, 6,* 19-22. https://doi.10.1002/asl.85
51. Strapazan, C., Haidu, I., & Kocsis, I. (2019). Assessing land use/land cover change and its impact on surface runoff in the southern part of the Țibleș and Rodnei Mountains. *Air and water components of the environment conference proceedings,* 225-236. https://doi.10.24193/AWC2019_23
52. Strapazan, C., Haidu, I., & Irimuș, I.-A. (2021). A comparative assessment of different loss methods available in Mike Hydro River – UHM. *Carpathian Journal of Earth and Environmental Sciences, 16*(1), 261 – 273. https://doi.10.26471/cjees/2021/016/172
53. Ștreang, O., Morar, C., & Roman, P. (2005). Utilizarea tehnicilor GIS în monitorizarea rapidă a cantităților de precipitații estimate cu radarul WSR 98D căzute în bazine hidrografice mici. *Sesiunea anuală de comunicări științifice* (pp. 73-80). INHGA, Bucuresti.
54. Tehrany, M., Pradhan, B., & Jebur, M. (2014). Flood susceptibility mapping using a novel ensemble weights-of-evidence and support vector machine models in GIS. *Journal of Hydrology, 512,* 332-343. https://doi.10.1016/j.jhydrol.2014.03.008
55. Universitatea Dimitrie Cantemir. (2013). *Hazard și risc în evaluarea și gestiunea resurselor naturale.* https://www.scribd. Com /doc/146056288/ managementul-RISCULUI (accessed on 5 April 2023).
56. Zaharia, L., Costache, R., Prăvălie, R., & Minea, G. (2015). Assessment and mapping of flood potential in the Slănic catchment in Romania. *Journal of Earth System Science, 124*(6), 1311-1324. https://doi.10.1007/s12040-015-0608-3
57. Zaharia, L., Costache, R., Prăvălie, R., & Toroimac, G. I. (2017). Mapping flood and flooding potential indices: a methodological approach to identifying areas susceptible to flood and flooding risk. Case study: the Prahova catchment (Romania). *Frontiers of Earth Science, 11(2).* https://doi.10.1007/s11707-017-0636-1
58. Zoccatelli, D., Borga, M., Zanon, F., Antonescu, B., & Stancalie, G. (2010). Which rainfall spatial information for flash flood response modelling? A numerical investigation based on data from the Carpathian range, Romania. *Journal of Hydrology, 394,* 148-161. https://doi.10.1016/j.jhydrol.2010.07.019